



Published in final edited form as:

*J Phys Chem Lett.* 2010 ; 1(19): 2936–2939. doi:10.1021/jz101159x.

## Unprecedented Fe(IV) Species in a Diheme Protein MauG: A Quantum Chemical Investigation on the Unusual Mössbauer Spectroscopic Properties

Yan Ling<sup>1</sup>, Victor L. Davidson<sup>2</sup>, and Yong Zhang<sup>1,3,\*</sup>

<sup>1</sup>Department of Chemistry and Biochemistry, University of Southern Mississippi, 118 College Drive #5043, Hattiesburg, MS 39406, USA

<sup>2</sup>Department of Biochemistry, University of Mississippi Medical Center, 2500 N. State Street, Jackson, MS 39216, USA

<sup>3</sup>Department of Chemistry, Chemical Biology, and Biomedical Engineering, Stevens Institute of Technology, Castle Point on Hudson, Hoboken, NJ 07030

### Abstract

Ferryl species are important catalytic intermediates in heme enzymes. A recent experimental investigation of a diheme protein MauG reported the first case of using two Fe(IV) species as an alternative to compound I in catalysis. Both Fe(IV) species have unusual Mössbauer properties, which was found to originate from novel structural features based on a quantum chemical investigation. With comparison to the previously reported Fe<sup>IV</sup>=O and Fe<sup>IV</sup>-OH species, results here provide the first evidence of a couple of new mechanisms by which proteins influence the properties of ferryl species by directly providing the O via Tyr, or stabilizing exogenous O via hydrogen bonding interaction. These results expand our ability to identify and evaluate high-valent heme proteins and models.

### Keywords

Fe(IV) species; heme; Mössbauer; DFT; hydrogen bond

High-valent Fe(IV) species are important intermediates in the catalytic cycles of many heme enzymes.<sup>1–9</sup> <sup>57</sup>Fe Mössbauer spectroscopy is an invaluable tool to probe iron sites and determine quadrupole splitting ( $\Delta E_Q$ ) and isomer shift ( $\delta_{Fe}$ ) parameters, which are related to the electric field gradient and charge density at the iron nucleus, respectively.<sup>4</sup> Fe(IV) species in heme proteins<sup>4–8</sup> are characterized by small  $\delta_{Fe}$  values ranging from 0.03–0.14 mm/s (Figure 1). In contrast,  $\Delta E_Q$  values<sup>4–8</sup> span a larger range of 1.02–2.29 mm/s. Thus,  $\Delta E_Q$  may be a more sensitive structural probe. Recent studies suggest that  $\Delta E_Q$  is an indicator of the protonation state of the oxo group,<sup>5,6,8</sup> with large and small  $\Delta E_Q$  values proposed for the protonated and unprotonated ferryl species, respectively. A model compound with an unprotonated Fe<sup>IV</sup>=O moiety<sup>9</sup> defined crystallographically has indeed a  $\Delta E_Q$  value (1.24 mm/s) at the lower end of this range.

\*Corresponding author: Yong Zhang zhangyuecedu@gmail.com.

Supporting Information Available: Computational details, optimized coordinates, and additional results (Tables S1–S12) are available free of charge via the Internet at <http://pubs.acs.org>.

MauG<sup>10</sup> contains two *c*-type hemes and catalyzes a six-electron oxidation to complete the biosynthesis of the tryptophan tryptophylquinone cofactor of methylamine dehydrogenase.<sup>11</sup> Mössbauer spectroscopy revealed that MauG stabilizes a bis-Fe<sup>IV</sup> intermediate with unusual  $\Delta E_Q$  values for each Fe<sup>IV</sup> heme.<sup>12</sup> Heme **1** was regarded as an Fe<sup>IV</sup>=O species, but its  $\Delta E_Q$  value of 1.70 mm/s lies between the average experimental  $\Delta E_Q$  values in heme proteins for protonated and unprotonated forms<sup>4–8</sup> (Figure 1). For heme **2**, both the  $\Delta E_Q$  and  $\delta_{Fe}$  values are larger than any previous known data for Fe(IV) species in heme proteins.<sup>12</sup> These results suggest that they may possess structural features that have not been described before. MauG is also the first known protein using two Fe<sup>IV</sup> centers as an alternative to compound I in biological oxidation reactions.<sup>12</sup>

Quantum chemical investigations of Mössbauer parameters have been useful in elucidating structural features of iron sites in proteins and models.<sup>13–22</sup> Here, we present a quantum chemical investigation of these two novel Fe<sup>IV</sup> species in heme proteins, using a recently determined MauG X-ray crystal structure<sup>23</sup> as a starting point. The DFT method used here has predicted  $\delta E_Q$  and  $\delta_{Fe}$  values in iron proteins and model systems covering all iron spin states and coordination states and almost all the iron oxidation states. The theory-versus-experiment correlation coefficient for  $\Delta E_Q$  prediction is  $R^2=0.98$  in 48 systems covering an experimental range of 8.80 mm/s and that for  $\delta_{Fe}$  prediction is  $R^2=0.97$  in 49 systems covering an experimental range of 2.34 mm/s (see Supporting Information for computational details). The standard deviation of these  $\delta_{Fe}$  calculations is 0.07 mm/s. It should be noted that our method was calibrated using the small molecules' X-ray structures and the residual errors were found to generally decrease upon using better quality X-ray structures.<sup>20</sup> For instance, the error in  $\Delta E_Q$  prediction for the ferryl model compound<sup>9</sup> that has a high resolution X-ray structure is 0.01 mm/s.<sup>21</sup> Therefore, this type of calculations has assisted in structure refinement for iron-containing proteins.<sup>20–22</sup> In this work, this approach was used to evaluate different Fe(IV) models in MauG.

Heme **1** is five-coordinate with a His residue as the axial ligand<sup>23</sup> and a vacant site to bind O<sub>2</sub> or H<sub>2</sub>O<sub>2</sub>. Five Fe<sup>IV</sup>-oxo models (**1a–1e** in Table 1) were investigated to examine the difference between the unprotonated Fe<sup>IV</sup>=O and protonated Fe<sup>IV</sup>-OH species, and possible hydrogen bonding effects from nearby amino acid residues. As found with the experimental studies,<sup>4–9,12</sup> the predicted  $\delta_{Fe}$  values in these models are similar and within the expected region, while  $\Delta E_Q$  values are much more sensitive to the structural variations.

As seen from Table 1, for the unprotonated Fe<sup>IV</sup>=O model **1a**, the predicted Fe-oxo distance and O-Fe-N<sub>His</sub> angle are similar to those seen in the X-ray structure of an Fe<sup>IV</sup>=O model compound (1.646 Å and 178.9°)<sup>9</sup> with a neutral N-coordination ligand similar to His investigated here. The predicted spin densities in Fe and O are also similar.<sup>21</sup> Its  $\Delta E_Q$  value of 1.45 mm/s is close to the average value of 1.4 mm/s seen for unprotonated Fe<sup>IV</sup>=O species in heme proteins (Figure 1). For the protonated Fe<sup>IV</sup>-OH model **1b**, the Fe-O distance and Fe spin density are similar to those of the Fe<sup>IV</sup>-OH species in heme proteins.<sup>5,6,8</sup> The 103% increase in  $\Delta E_Q$  caused by protonation of the oxo group (see Table 1 for results of **1b** vs. **1a**) is comparable to an average increase of 112% in other heme proteins.<sup>5,6,8</sup>

It can be seen from Table 1 that the experimental  $\Delta E_Q$  value of MauG heme **1** lies between the  $\Delta E_Q$  values of the protonated Fe<sup>IV</sup>-OH model **1b** and the unprotonated Fe<sup>IV</sup>=O model **1a**, and is closer to the latter one. This suggests that a secondary effect from nearby residue(s) may operate on the unprotonated Fe<sup>IV</sup>=O species in MauG heme **1**. Therefore, models **1c–1e** were built on the basis of the unprotonated Fe<sup>IV</sup>=O model which includes residues Gln103 and Pro107 that reside near heme **1** in the crystal structure to investigate such effects. Model **1c** includes only Gln103 with its terminal N-H hydrogen bonded to the oxo group of the ferryl moiety (see Supporting Information for computational details). Interestingly, as shown in Table

1, this hydrogen bond reduces the error in the  $\delta E_Q$  prediction from 0.25 mm/s in **1a** to 0.11 mm/s in **1c**. The error can be further reduced to be 0.03 mm/s in **1d** (see Figure 2A), if Gln103 is allowed to move with no constraints from the resting state X-ray structure to further optimize its interaction with the  $\text{Fe}^{\text{IV}}=\text{O}$  group. This kind of hydrogen bond effect is similar to the  $\Delta E_Q$  changes of 0.1–0.2 mm/s reported previously in other heme protein systems.<sup>8,24</sup> Results here suggest for the first time that an  $\text{Fe}(\text{IV})=\text{O}$  species may be stabilized by an active site residue, which in MauG was experimentally found to be remarkably stable.<sup>12</sup> It is also intriguing that the alignment of the amino acid sequences of MauG proteins indicates that Gln103 is absolutely conserved (see Figure S2 in reference 23). These results suggest that Gln103 may play a functional role in this site, which will be further investigated by mutation studies. In contrast to Gln103, the presence of Pro107 in **1e** compared to **1c** has minimal effects on the geometries, spin densities, and Mössbauer parameters. Thus, the role of Pro107 is likely structural and perhaps related to the fact that MauG does not require substrate binding to prime it for reactions with oxygen.<sup>23</sup> These results suggest that quantum chemical studies of characteristic spectroscopic properties for proteins may help identify the roles of active site residues.

For heme **2**, the MauG X-ray structure reveals an unusual His/Tyr ligation.<sup>23</sup> It has never been observed for *c*-type hemes or any other heme proteins where function requires the formation of an  $\text{Fe}^{\text{IV}}$  oxidation state. In principle, three major types of  $\text{Fe}^{\text{IV}}$  hemes may be formed upon the binding of  $\text{O}_2$  or  $\text{H}_2\text{O}_2$  to MauG: 1) His- $\text{Fe}^{\text{IV}}-\text{O}(\text{H})$  (**2a** and **2b**); 2)  $(\text{H})\text{O}-\text{Fe}^{\text{IV}}-\text{Tyr}$  (**2c** and **2d**); 3) His- $\text{Fe}^{\text{IV}}-\text{Tyr}$  (**2e**). However, as shown in Table 1, for type 1 and 2 models, either  $\Delta E_Q$  or  $\delta_{\text{Fe}}$  predictions have much large errors compared to the experimental data, which supports the proposal in the original experimental investigation of MauG that this  $\text{Fe}^{\text{IV}}$  heme site has two protein residues as axial ligands.<sup>12</sup> To examine the consequence of an  $\text{Fe}^{\text{IV}}$  heme with the unique His/Tyr ligand set (type 3), model **2e** of  $\text{Fe}^{\text{IV}}(\text{Por})^{2-}(\text{His})^0(\text{Tyr})^{1-}$  was investigated (Figure 2B). The average Fe and porphyrin nitrogen distance ( $R_{\text{FeN-Por}}$ ) in **2e** is similar to the values of 2.01–2.03 Å seen in the isoelectronic  $\text{Fe}^{\text{IV}}-\text{OH}$  species in previously studied heme proteins<sup>6</sup> and the  $\text{Fe}^{\text{IV}}-\text{OH}$  heme model (**1b**) here. The long Fe-O bond length of 1.839 Å in **2e** is similar to the Fe-O bond (1.84 Å) in a model compound,<sup>8</sup>  $\text{Fe}^{\text{IV}}(\text{TMP})(\text{OCH}_3)_2$  (TMP = tetramesitylporphyrin), with the same coordinate state and a similarly high  $\Delta E_Q$  value of 2.12 mm/s.<sup>25</sup> It should be noted that the  $\text{Fe}^{\text{IV}}-\text{OCH}_3$  group is isoelectronic to a  $\text{Fe}^{\text{IV}}-\text{OH}$  species. So, the  $\Delta E_Q$  value of  $\text{Fe}^{\text{IV}}(\text{TMP})(\text{OCH}_3)_2$  is close to the  $\Delta E_Q$  value of 2.06–2.29 mm/s seen with the  $\text{Fe}^{\text{IV}}-\text{OH}$  species in other heme proteins.<sup>5,6,8</sup>

A notable difference from the previously investigated  $\text{Fe}^{\text{IV}}=\text{O}$  and  $\text{Fe}^{\text{IV}}-\text{OH}$  heme species is that the Mulliken spin densities of the oxo and iron atoms ( $\rho_{\alpha\beta}^{\text{O}}$  and  $\rho_{\alpha\beta}^{\text{Fe}}$ ) in **2e** are ca. 0.5 e smaller than the two electrons expected for an  $S=1$  state. However, the spin densities of the whole Tyr group and Fe of 1.92 e are indeed close to the expected value, suggesting a delocalization effect of the conjugated Tyr residue. Compared to the  $\text{Fe}^{\text{IV}}-\text{OH}/\text{OCH}_3$  species reported before<sup>5,6,8,25</sup> that have dual anionic axial ligands, the unique ligand set of His/Tyr makes **2e** isoelectronic to **1b**, which also has one neutral His axial ligand and one anionic axial ligand. Note that **1b** has a  $\Delta E_Q$  value larger than those of previously reported  $\text{Fe}^{\text{IV}}-\text{OH}/\text{OCH}_3$  species, which is the same for **2e**. Since Tyr has only one formal negative charge, which is smaller than the two formal negative charges for an oxo group, **2e** has a much longer Fe-O bond compared to those in other  $\text{Fe}^{\text{IV}}$ -oxo porphyrins investigated here (see Table 1) and previously.<sup>4–8</sup> This decreases the electron charge density at the iron nucleus, which is negatively proportional to  $\delta_{\text{Fe}}$  and thus results in a much large  $\delta_{\text{Fe}}$  value.<sup>4</sup> To further examine the effect of this unique Tyr/His ligand set on Mössbauer parameters, a calculation of  $\text{Fe}^{\text{IV}}(\text{Por})^{2-}(\text{His})^0(\text{Tyr})^{1-}$  using a simple non-substituted porphyr with no protein structural restraints (**2f**) was performed. As seen from Table 1, both the geometric and Mössbauer results are not identical to those of **2f**, indicating an effect of the protein environment. However, both  $\Delta E_Q$  and  $\delta_{\text{Fe}}$  values of **2f** are again much larger than those reported previously, which further

supports an important role of the His/Tyr ligand set in determining the unusually large Mössbauer parameters. These results support for a novel Fe<sup>IV</sup> protein state without an exogenous non-protein ligand.

Overall, the geometric, electronic, and Mössbauer properties from this work suggests new mechanisms by which proteins influence the properties of Fe<sup>IV</sup>=O hemes by directly providing the O via Tyr, or stabilizing exogenous O via hydrogen bonding interaction. These results expand our ability to identify and evaluate high-valent heme proteins and models.

## Supplementary Material

Refer to Web version on PubMed Central for supplementary material.

## Acknowledgments

This work was supported by the NIH grants GM-085774 (YZ) and GM-41574 (VLD). We thank Mississippi Center for Supercomputing research and USM Vislab for using the computing facilities and Lyndal M. R. Jensen and Carrie M. Wilmot for providing the coordinates prior to publication and helpful discussions, and Aimin Liu for his assistance.

## References

- (1). Dawson JH. Probing Structure-function Relations in Heme-containing Oxyganses and Peroxidases. *Science* 1988;240:433–439. [PubMed: 3358128]
- (2). Schlichting I, Berendzen J, Chu K, Stock AM, Maves SA, Benson DE, Sweet BM, Ringe D, Petsko GA, Sligar SG. The Catalytic Pathway of Cytochrome P450cam at Atomic Resolution. *Science* 2000;287:1615–1622. [PubMed: 10698731]
- (3). Shaik S, de Visser SP, Kumar D. One Oxidant, Many Pathways: A Theoretical Perspective of Monooxygenation Mechanisms by Cytochrome P450 enzymes. *J. Biol. Inorg. Chem* 2004;9:661–668. [PubMed: 15365903]
- (4). Debrunner, PG. Iron Porphyrins. Lever, ABP.; Gray, HB., editors. Vol. Vol. 3. VCH Publishers; New York: 1989. p. 139-234.
- (5). Stone KL, Hoffart LM, Behan RK, Krebs C, Green MT. Evidence for Two Ferryl Species in Chloroperoxidase Compound II. *J. Am. Chem. Soc* 2006;128:6147–6153. [PubMed: 16669684]
- (6). Behan RK, Hoffart LM, Stone KL, Krebs C, Green MT. Evidence for Basic Ferryls in Cytochromes P450. *J. Am. Chem. Soc* 2006;128:11471–11474. [PubMed: 16939270]
- (7). Garcia-Serres R, Davydov RM, Matsui T, Ikeda-Saito M, Hoffman BM, Huynh BH. Distinct Reaction Pathways Followed upon Reduction of Oxy-heme Oxygenase and Oxy-myoglobin as Characterized by Mossbauer Spectroscopy. *J. Am. Chem. Soc* 2007;129:1402–1412. [PubMed: 17263425]
- (8). Horner O, Mouesca JM, Solari PL, Orio M, Oddou JL, Bonville P, Jouve HM. Spectroscopic Description of an Unusual Protonated Ferryl Species in the Catalase from *Proteus mirabilis* and Density Functional Theory Calculations on Related Models. Consequences for the Ferryl Protonation State in Catalase, Peroxidase and Chloroperoxidase. *J. Biol. Inorg. Chem* 2007;12:509–525. [PubMed: 17237942]
- (9). Rohde, JU.; In, JH.; Lim, MH.; Brennessel, WW.; Bukowski, MR.; Stubna, A.; Munck, E.; Nam, W.; Que, L. *Science*. Vol. 299. 2003. Crystallographic and Spectroscopic Characterization of a Nonheme Fe(IV)=O Complex; p. 1037-1039.
- (10). Wang YT, Graichen ME, Liu AM, Pearson AR, Wilmot CM, Davidson VL. MauG, a Novel Diheme Protein Required for Tryptophan Tryptophylquinone Biogenesis. *Biochemistry* 2003;42:7318–7325. [PubMed: 12809487]
- (11). Wilmot CM, Davidson VL. Uncovering Novel Biochemistry in the Mechanism of Tryptophan Tryptophylquinone Cofactor Biosynthesis. *Curr. Opin. Chem. Biol* 2009;13:469–474. [PubMed: 19648051]
- (12). Li XH, Fu R, Lee SY, Krebs C, Davidson VL, Liu AM. A Catalytic Di-heme Bis-Fe(IV) Intermediate, Alternative to an Fe(IV)=O Porphyrin Radical. *Proc. Natl. Acad. Sci. U. S. A* 2008;105:8597–8600. [PubMed: 18562294]

- (13). Han WG, Liu TQ, Lovell T, Noodleman L. Active Site Structure of Class I Ribonucleotide Reductase Intermediate X: A Density Functional Theory Analysis of Structure, Energetics, and Spectroscopy. *J. Am. Chem. Soc* 2005;127:15778–15790. [PubMed: 16277521]
- (14). Lovell T, Han WG, Liu TQ, Noodleman L. A Structural Model for the High-valent Intermediate Q of Methane Monooxygenase from Broken-symmetry Density Functional and Electrostatics Calculations. *J. Am. Chem. Soc* 2002;124:5890–5894. [PubMed: 12010064]
- (15). Sinnecker S, Svensen N, Barr EW, Ye S, Bollinger JM, Neese F, Krebs C. Spectroscopic and Computational Evaluation of the Structure of the High-spin Fe(IV)-oxo Intermediates in Taurine: Alpha-Ketoglutarate Dioxygenase from *Escherichia coli* and its His99Ala Ligand Variant. *J. Am. Chem. Soc* 2007;129:6168–6179. [PubMed: 17451240]
- (16). Schoneboom JC, Neese F, Thiel W. Toward Identification of the Compound I Reactive Intermediate in Cytochrome P450 Chemistry: A QM/MM Study of its EPR and Mossbauer Parameters. *J. Am. Chem. Soc* 2005;127:5840–5853. [PubMed: 15839682]
- (17). Neese F. Prediction and Interpretation of the Fe-57 Isomer Shift in Mossbauer Spectra by Density Functional Theory. *Inorg. Chim. Acta* 2002;337:181–192.
- (18). Grodzicki M, Flint H, Winkler H, Walker FA, Trautwein AX. Electronic Structure, Porphyrin Core Distortion, and Fluxional Behavior of Bis-ligated Low-spin Iron(II) Porphyrinates. *J. Phys. Chem. A* 1997;101:4202–4207.
- (19). Chanda A, Shan XP, Chakrabarti M, Ellis WC, Popescu DL, de Oliveira FT, Wang D, Que L, Collins TJ, Munck E, Bominaar EL. (TAML)Fe-IV=O Complex in Aqueous Solution: Synthesis and Spectroscopic and Computational Characterization. *Inorg. Chem* 2008;47:3669–3678. [PubMed: 18380453]
- (20). Zhang Y, Gossman W, Oldfield E. A Density Functional Theory Investigation of Fe-N-O Bonding in Heme Proteins and Model Systems. *J. Am. Chem. Soc* 2003;125:16387–16396. [PubMed: 14692781]
- (21). Zhang Y, Oldfield E. Cytochrome P450: An Investigation of the Mossbauer Spectra of a Reaction Intermediate and an Fe(IV)=O Model System. *J. Am. Chem. Soc* 2004;126:4470–4471. [PubMed: 15070336]
- (22). Zhang Y, Oldfield E. On the Mossbauer Spectra of Isopenicillin N Synthase and a Model {FeNO} (7) (S=3/2) System. *J. Am. Chem. Soc* 2004;126:9494–9495. [PubMed: 15291525]
- (23). Jensen LMR, Sanishvili R, Davidson VL, Wilmot CM. In Crystallo Posttranslational Modification within a MauG/pre-methylamine Dehydrogenase Complex. *Science* 2010;327:1392–1394. [PubMed: 20223990]
- (24). Ling, Y.; Zhang, Y. *Annual Reports in Computational Chemistry*. Wheeler, RA., editor. Vol. Vol. 6. Elsevier; New York: 2010. p. 65-77.
- (25). Groves JT, Quinn RQ, Mc Murry TJ, Nakamura M, Lang G, Boso B. Preparation and Characterization of a Dialkoxyiron (IV) Porphyrin. *J. Am. Chem. Soc* 1985;107:354–360.

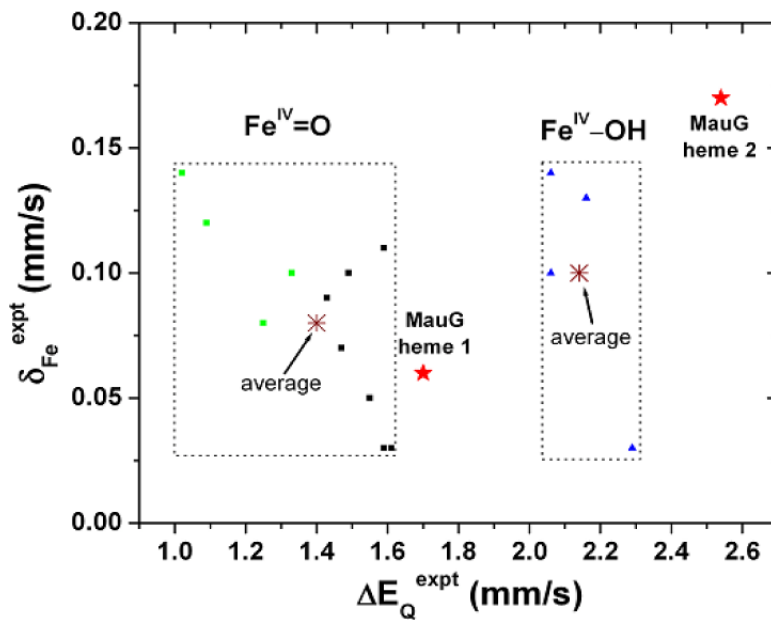


**Figure 1.** Experimental Mössbauer properties for Fe(IV) heme proteins.<sup>4–8,12</sup> Green squares, black squares, and blue triangle points are for compounds I  $\text{Fe}^{\text{IV}}=\text{O}$ , compound II/ES  $\text{Fe}^{\text{IV}}=\text{O}$ , and compound II  $\text{Fe}^{\text{IV}}-\text{OH}$  species, respectively.

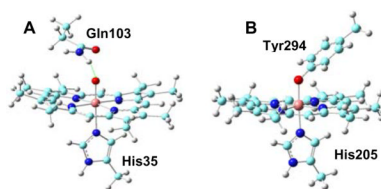


**Figure 2.** Active site models of MauG Fe<sup>IV</sup> heme sites: (A) **1d**; (B) **2e**. The green dotted line in (A) represents a hydrogen bond.

**Table 1**  
Geometric, Electronic, and Mössbauer Properties of MauG Fe(IV) Models (S=1)

MauG models <sup>a</sup>	R <sub>FeO</sub> (Å)	R <sub>FeN-His</sub> (Å)	R <sub>FeO-Tyr</sub> (Å)	R <sub>FeN-Por</sub> (Å)	∠O-Fe-N <sub>His</sub> (degrees)	ρ <sub>up</sub> <sup>Fe</sup> (e)	ρ <sub>up</sub> <sup>O</sup> (e)	ΔE <sub>q</sub> (mm/s)	δ <sub>Fe</sub> (mm/s)
<b>heme 1</b>	Exptl <sup>b</sup>							1.70	0.06
<b>1a:</b> Fe <sup>IV</sup> (Por) <sup>2-</sup> (His) <sup>0</sup> (O) <sup>2-</sup>	Calcd	2.333	/	2.042	176.6	1.18	0.89	1.45	0.15
<b>1b:</b> Fe <sup>IV</sup> (Por) <sup>2-</sup> (His) <sup>0</sup> (OH) <sup>1-</sup>	Calcd	2.202	/	2.032	175.3	1.99	0.09	2.95	0.10
<b>1c:</b> Fe <sup>IV</sup> (Por) <sup>2-</sup> (His) <sup>0</sup> (O...HB1) <sup>2-</sup>	Calcd	2.328	/	2.042	176.0	1.25	0.83	1.59	0.14
<b>1d:</b> Fe <sup>IV</sup> (Por) <sup>2-</sup> (His) <sup>0</sup> (O...HB1) <sup>2-</sup>	Calcd	2.330	/	2.043	176.2	1.27	0.80	1.67	0.13
<b>1e:</b> Fe <sup>IV</sup> (Por) <sup>2-</sup> (His) <sup>0</sup> (O...HB2) <sup>2-</sup>	Calcd	2.290	/	2.044	177.2	1.28	0.79	1.55	0.13
<b>heme 2</b>	Exptl <sup>b</sup>							2.54	0.17
<b>2a:</b> Fe <sup>IV</sup> (Por) <sup>2-</sup> (His) <sup>0</sup> (O) <sup>2-</sup>	Calcd	2.125	/	2.031	177.8	1.13	0.94	0.84	0.13
<b>2b:</b> Fe <sup>IV</sup> (Por) <sup>2-</sup> (His) <sup>0</sup> (OH) <sup>1-</sup>	Calcd	2.042	/	2.021	177.6	1.85	0.16	2.58	0.03
<b>2c:</b> Fe <sup>IV</sup> (Por) <sup>2-</sup> (Tyr) <sup>1-</sup> (O) <sup>2-</sup>	Calcd	1.677	2.027	2.037	175.5	1.18	0.88	0.51	0.17
<b>2d:</b> Fe <sup>IV</sup> (Por) <sup>2-</sup> (Tyr) <sup>1-</sup> (OH) <sup>1-</sup>	Calcd	1.815	1.882	2.033	176.3	1.65	0.15	1.79	0.11
<b>2e:</b> Fe <sup>IV</sup> (Por) <sup>2-</sup> (His) <sup>0</sup> (Tyr) <sup>1-</sup>	Calcd	/	1.839	2.010	177.3	1.25	0.30	2.48	0.24
<b>2f:</b> Fe <sup>IV</sup> (Por) <sup>2-</sup> (His) <sup>0</sup> (Tyr) <sup>1-</sup>	Calcd	2.016	1.839	2.005	174.9	1.18	0.37	2.75	0.24

See Text for HB1<sup>a</sup>, Por<sup>a</sup>, His<sup>a</sup>, and Tyr<sup>a</sup>.

<sup>a</sup>Por, HB1, and HB2 stand for the porphyrin structure, Gln103, and Gln103/Pro107 residues.

<sup>b</sup>Ref. 12.